JOURNAL OF OPTOELECTRONICS AND ADVANCED MATERIALS Vol. 12, No. 12, December 2010, p. 2380 - 2385

Barium magnesium tantalate thin films deposited by RF-magnetron sputtering from a stoichiometric target

V. BRAIC*, A. KISS, A. IOACHIM[a], M. TOACSAN[a], L. NEDELCU[a], M. BRAIC
National Institute for Optoelectronics, P.O.Box MG 5, Bucharest-Magurele, Romania
[a]National Institute for Materials Physics, P.O.Box MG 7, Bucharest-Magurele, Romania

Barium magnesium tantalate thin films are attractive materials for high-performance dielectric ceramics for microwave devices, exhibiting a high dielectric constant, a low loss and a near-zero temperature coefficient. We report on the successful deposition of polycrystalline barium magnesium tantalate thin films by RF magnetron sputtering method. The structural and morphological characterization data are presented.

(Received November 11, 2010; accepted November 25, 2010)

Keywords: Ceramic films, RF magnetron sputtering, Crystallographic structure, Elemental composition, Films' morphology

1. Introduction

There is a growing interest in the development of high-performance dielectric ceramics for microwave devices, requiring a high dielectric constant, a low loss and a near-zero temperature coefficient [1, 2]. The complex perovskite materials, $Ba(Mg_{1/3}Ta_{2/3})O_3$ (BMT) and $Ba(Zn_{1/3}Ta_{2/3})O_3$, have been reported to have excellent microwave dielectric properties [3, 4]. In the microwave domain, the bulk BMT ceramic is characterized by very low dielectric loss, high dielectric constant, and a very good stability with temperature [5, 6]. Magnesium loss in BMT compounds generate a family of compounds with the formula $Ba_6Mg_{0.67}Ta_{9.33}O_{30}$, presenting lower permittivity and losses, but which can be successfully used in microwave applications [7], e.g. as microwave resonators [8].

In this work, we report on the preparation and characterization of barium magnesium tantalate thin films by RF magnetron sputtering method. To date, BMT films are reported to be obtained by PLD [9] or sol – gel methods [10, 11], no data being available for magnetron deposition of such films, probably related to the difficulties in obtaining complex ceramic films by this method. The aim of this work is to investigate the influence of the substrate temperature during film growth and of the annealing parameters on the films' crystallographic structure, composition and morphology.

2. Experimental details

Proportionate amounts of reagent-grade starting materials of $BaCO_3$, MgO and Ta_2O_5 were mixed, according to the stoichiometric composition of $Ba(Mg_{1/3}Ta_{2/3})O_3$ and ball-milled for 2 h with distilled water. After 24 h drying at T = 200^{0}C, the reagents were again ball-milled for 2 h in an agate mortar and afterwords the powders were calcined for 2 h at 1250 ^{0}C. After calcination, the powders were ball-milled again for 5 h and dryied for 12 h at 80^{0}C and then pressed uniaxially into pellets in a steel die and sintered at 1650^{o}C under ambient conditions for a duration of 4 h, in order to obtain a stoichiometric $Ba(Mg_{0.33}Ta_{0.67})O_3$ ceramic target, which was used as cathode for thin films deposition. The crystallographic structure of the resulting target was examined by XRD.

The ceramic thin films were obtained using an RF magnetron sputtering (13.56 MHz) system equipped with three cathodes (2.54 cm diameter). The base pressure in the deposition chamber was of about $1x10^{-5}$ Pa. The absolute pressure was measured with a MKS 626 Barocel capacitance manometer. A stoichiometric $Ba(Mg_{0.33}Ta_{0.67})O_3$ ceramic target was used as cathode.

The ceramic films were deposited on Si substrates. Prior to deposition, the substrates were chemically cleaned in an ultrasonic bath with isopropyl alcohol. Both the substrates and the magnetron target were sputter cleaned in vacuum by Ar ion bombardment for 10 minutes, in order to remove any residual impurities.

The films were deposited at three different substrate temperatures: 100ºC - samples S_1, 700ºC - sample S_2 and 800ºC - sample S_3, continuously monitored by a backside non contact thermocouple. During the deposition process the total pressure was kept constant (7.10^{-1} Pa). The films were deposited in Ar atmosphere. During the deposition the substrate was RF biased at an equivalent voltage of -100 V. The RF power delivered to the ceramic cathode was 40 W. The deposition time was set at 90 minutes. The as-deposited thin films were annealed in air for different time periods, at 850^{0}C and 900^{0}C. The annealing period is referring to the time period when the temperature was maintained constant. The samples were heated either with a temperature gradient $\nabla T_{annealing}$ = 25^{0}C/min, or instantly, being introduced directly in the pre-heated oven. The both annealing treatments were followed by free cooling. Experimental conditions for the annealing conditions of films are presented in Table 1. The analyzed samples will be nominated as S_iA_j.

Table 1. Annealing conditions (Aj) of the deposited ceramic films.

Annealing conditions	$T_{annealing}$ (^{0}C)	$\nabla T_{annealing}$ (^{0}C/min)	$t_{annealing}$ (min)
A_1	850	25	20
A_2	900	25	0
A_3	900	25	1
A_4	900	25	2
A_5	900	25	4
A_6	900	25	20
A_7	900	∞	20

The bulk density of the ceramics was measured by the water immession Archimedes method, using a picnometer device at room temperature. The dielectric parameters of BMT bulk samples were investigated by using the Hakki-Coleman method, using a computer-aided measurement system, comprising an HP 8757C network analyzer and an HP 8350B sweep oscillator [12].

The XRD measurements have been performed using a Bruker-D8 Advance type X-ray diffractometer, equipped with a copper target X-ray tube, and a scintillation detector. For thin film measurements, a parallel beam geometry at grazing incidence $\alpha = 2^0$ was used, with a Göbel mirror in the incident beam. An asymmetric channel cut installed after the mirror provided a strictly monochromatic $CuK_{\alpha 1}$ primary X-ray beam.

XPS was used to identify the elemental films composition using a VG ESCA 3 MK II spectrometer using monochromatized Al K_α radiation (1486.6 eV). The spectra were processed using Spectral Data Processor v 2.3 software [13]. Before investigation the surface of the samples was sputter-cleaned with 1 keV Ar ion gun for 5 minutes [14].

Film thickness, surface roughness and morphology were assessed with Veeco's Dektak 150 surface profiler and Veeco - Innova scanning probe microscope (SPM) operating in tapping mode, respectively. SEM images of the films surface and fracture were obtained by using a JEOL Nova 400 NanoSEM microscope.

3. Results and discussion

The measured bulk density of the BMT ceramics was $\rho_r = 7.38$ g/cm^3, indicating a densification percentage of about 96.9% from the theoretical density, which corresponds to an intergranular total porosity of 3.1%.

The XRD pattern of the bulk BMT ceramic indicate a single phase compound, well crystallised in a hexagonal structure (JCPDS card no. 70-9201), with the chemical formula $Ba(Mg_{0.33}Ta_{0.67})O_3$, without secondary phases (Fig.1). The SEM image (Fig. 2) presents some morphologic aspects of the bulk ceramic sample, with well faceted polyhedral grains, and the size in the range 2 - 10 μm, with few sub-micron grains, evidentiated on the large surfaces of the ceramic grains. The porous structure is represented by few intergranular pores with dimensions in the same range as the grains.

The measured dielectric constant of the bulk BMT sample is ε = 24, with a very low value of the dielectric loss ($\tan\delta = 3.4 \times 10^{-5}$).

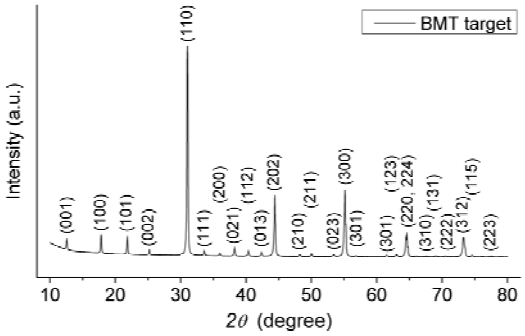

Fig. 1 X-ray diffraction patterns of BMT target sintered at 1650^{0}C/ 4h.

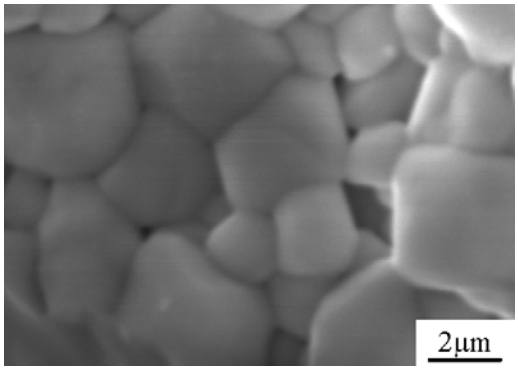

Fig. 2. SEM image within a fracture of the BMT target.

The thickness of the films were approx. 650 nm, with small variations of about 10%. The XRD measurements revealed that all the as deposited ceramic films were amorphous, disregarding the deposition temperature. The films' crystallization took place only at 900^{0}C annealing temperature, for A_1 annealing condition the S_1 - S_3 films remaining amorphous. Some representative XRD spectra are presented in Fig. 3. As identified from JCPDS 056-0398, the films crystallized in a tetragonal structure, corresponding to the chemical formula $Ba_6Mg_{0.67}Ta_{9.33}O_{30}$.

Comparing the presented XRD spectra of the samples S_1A_7 and S_2A_7, it clearly results that the deposition temperature has no influence on the films' crystallographic structure obtained after the A_7 annealing process. Considering the A_6 annealing condition, the XRD spectra of the $S_{1\text{-}3}A_6$ samples (only S_1A_6 spectrum shown here) are practically indistinguishable from the spectra $S_{1\text{-}3}A_7$, pointing out that the crystallographic structure is depending only on the annealing time, different heating gradients having no influence on the observed structure. In the XRD spectra there are also evidentiated secondary, unknown phases, which were not possible to be ascribed to the Ba, Ta or Mg oxides or sub-oxides.

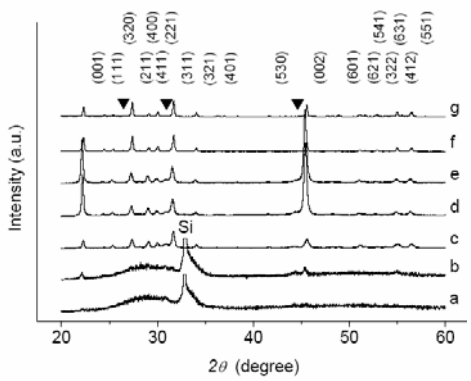

Fig. 3. X-ray diffraction patterns for the films annealed for different time periods, where ▾ represents unascribed, secondary phases (samples a - S_1A_2, b - S_1A_3, c - S_1A_4, d - S_1A_5, e - S_1A_6, f - S_1A_7 and g- S_2A_7)

As it can be seen, the films' texture was continuously modified as the annealing duration increases. The films start to crystallize during the heating period, but only after 1 minute annealing few small peaks became visible, corresponding to the (001), (002) and (412) planes. As the annealing duration is increasing, many more maxima appear, their number remaining practically unchanged after 2 minutes of annealing.

The mean crystallite size (D) in the tetragonal BMT films was calculated from the broadening of the (311) line using the Scherrer formula: $D = k\lambda / \beta \cos\theta$, where β is the full width at half maximum, θ is the Bragg angle, and k=0.9. The entire peak broadening was attributed only to the crystallite size effect. The line width was corrected for instrumental broadening using a corundum reference sample.

In Table 2 are presented the D values as a function of deposition temperature and annealing treatment. For a certain annealing condition (A_6 and A_7), the D parameter increase as the films' growth temperature is increasing, indicates a better crystallization process. For the S_1 films, as the annealing time is increasing, the D parameter also increases, indicating, as expected, the importance of the annealing duration for the crystallization process. The D parameter presents the highest values for the films undergoing the A_7 annealing process, indicating this one as an optimal one for obtaining crystalline films.

The calculated lattice parameters for the tetragonal phase, shown in Table 2, present larger values than those extracted from JCPDS 056-0398 (a_{JCPDS} = 12.61810 Å; c_{JCPDS} = 3.96720 Å), indicating the inflation of the unit cell, due to the replacement of smaller (Ba or Mg) atoms with the larger Ta atoms. For the annealing conditions A_1-A_6, it was evidenced an inflation of the unit cell which is proportional to the annealing duration. However, with no pre-heating (condition A_7) it was observed a smaller inflation of the unit cell, corresponding to "c" parameter, along with a shrinking of the unit cell corresponding to the "a" parameter. These values, more near to the ideal ones, as well as the increase of mean crystallite size, indicate that a higher deposition temperature favors the growth of the tetragonal crystalline phase under subsequent annealing, even if the as deposited films are amorphous.

The ratios of different elements concentrations, as derived from XPS analyses, are presented in Fig. 5, for the ceramic cathode used in the deposition process, for different films, before and after annealing, and also for an "ideal" BMT ceramic. It is obvious that the annealing process is determining a loss of Ba, resulting in a Ta excess. The observed Ba deficiency in the investigated films, as compared to the stoichiometric BMT, is consistent with the formation of tetragonal phase, as determined by XRD measurement. Also, the deposition of films at higher temperatures determines a more pronounced loss of Ba atoms. In Fig. 6 are presented the XPS Ba5d3 (778.4 eV) and Ta4f5 (27.7 eV) / Ta 4f7 (25.8 eV) spectra of the D_1A_7 [15-19].

Table 2. Mean crystallite size (D) and the unit cell parameter (a, c), as a function of deposition and annealing parameters

Sample	S_1A_4	S_1A_5	S_1A_6	S_1A_7	S_2A_6	S_2A_7	S_3A_6
D (nm)	30	36	42	48	45	59	47
a (Å)	12.626	12.652	12.656	12.603	12.657	12.592	12.660
$\Delta a = a - a_{JCPDS}$ (Å)	0.0079	0.0339	0.0379	-0.0151	0.0389	-0.0261	0.0419
c (Å)	3.977	3.992	3.994	3.978	3.996	3.976	3.998
$\Delta c = c - c_{JCPDS}$ (Å)	0.0098	0.0248	0.0268	0.0108	0.0288	0.0088	0.0308

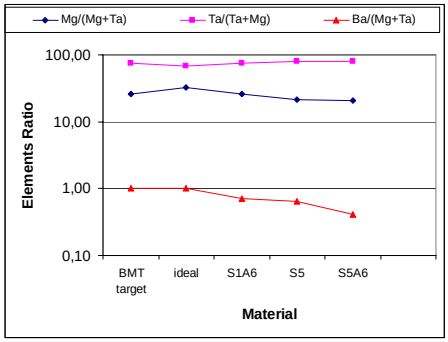

Fig. 5. The ratios of different elements concentrations, as derived from XPS analyses.

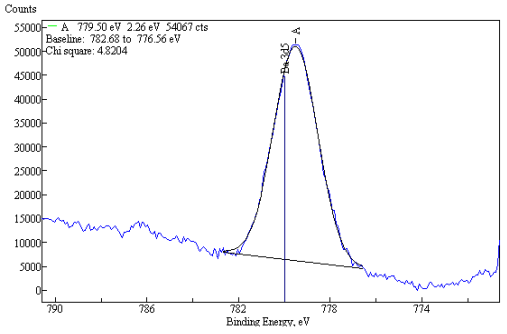

Fig. 6a XPS Ba5d spectrum of the sample S_1A_7.

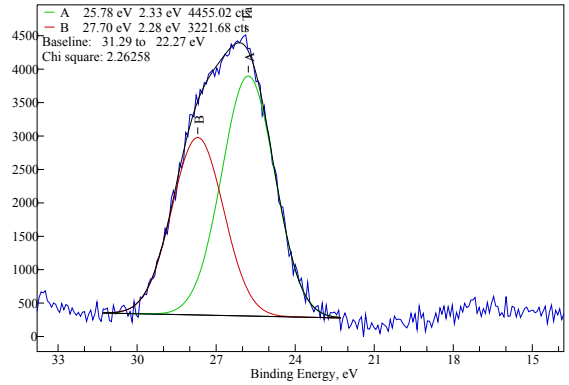

Fig. 6b XPS Ta4f spectrum of the sample S_1A_7.

In Figs. 7a-f are presented some AFM images of the samples, while in Table 4 are presented the corresponding RMS values. The as deposited films have a low roughness, which increases with the deposition temperature and after annealing, as usually observed in oxides [20] and oxynitrides [21]. For the S_1 films deposited at 100 ^{0}C, the surfaces present a gradual increase of the roughness with the duration of the annealing treatment, due to film crystallization and growth of the grain dimensions (Figs. 7 b-d). The lower roughness was obtained for the amorphous, as deposited film (Fig. 7a). It is worth to note that the films annealed under A_7 condition present a much lower roughness than the films annealed, for the same period, under A_6 condition. This can be ascribed to the rapid crystallization process which takes place under A_7 condition, compared with a longer heating period preceding the crystallization process undergone by the films annealed under A_6 condition. The increase of the deposition temperature induces a higher surface roughness, as presented in Fig. 7f, as compared to Fig. 7d.

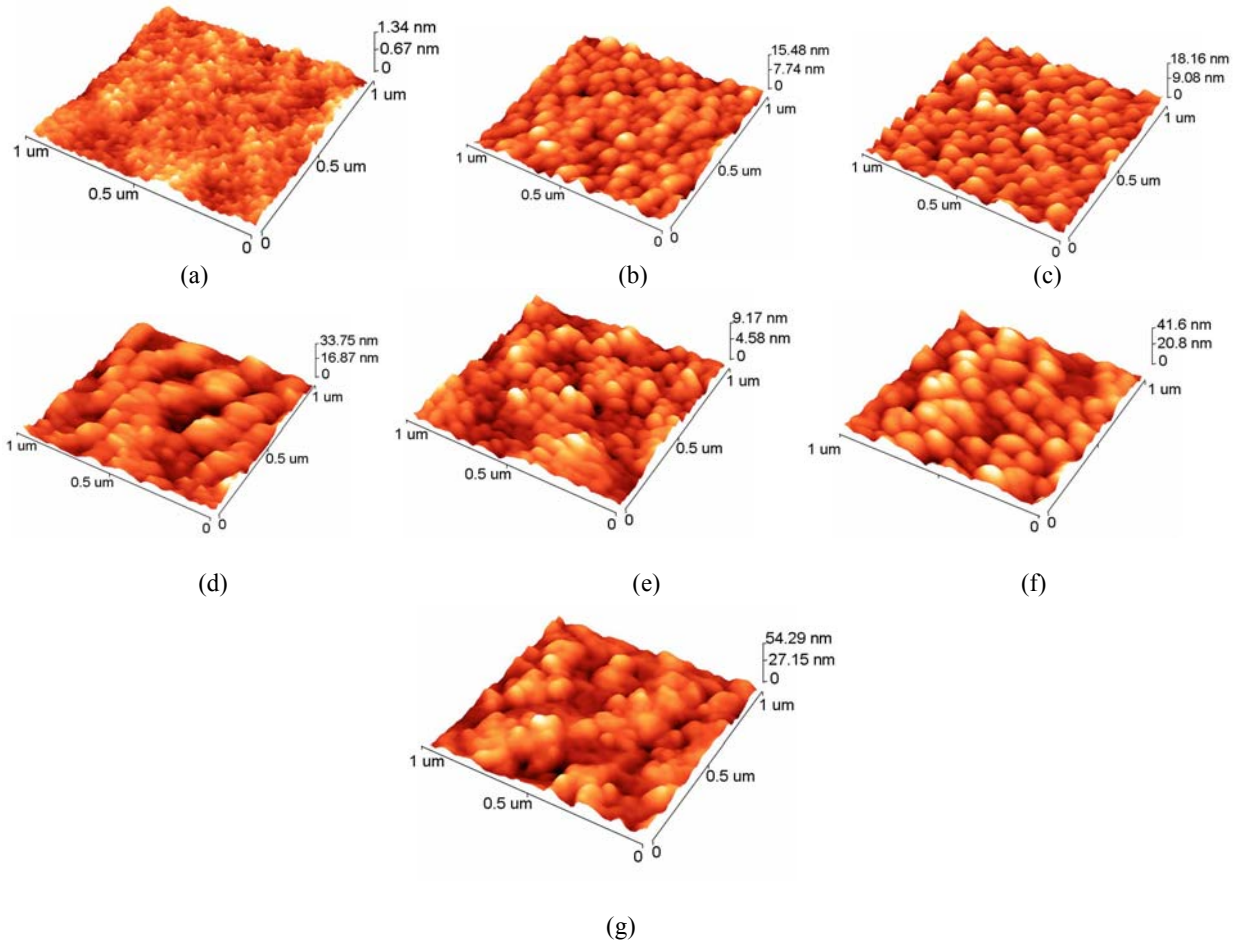

Fig. 7. AFM images of different non-stoichiometric BMT films, samples (a) - S_1, (b) - S_1A_4, (c) - S_1A_5, (d) -S_1A_6, (e) - S_1A_7, (f) - S_2A_6 and (g) - S_3A_6

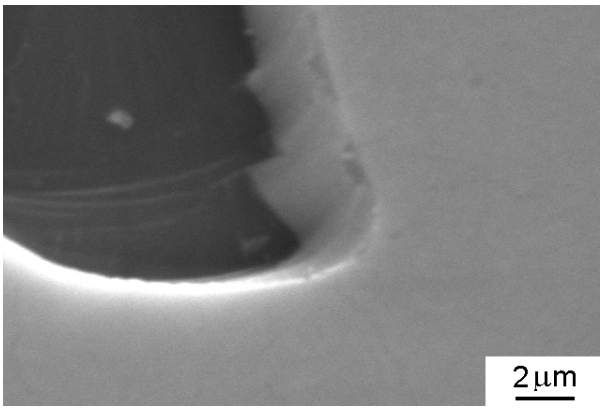

Fig. 8. SEM cross section through a $Ba_6Mg_{0.67}Ta_{9.33}O_{30}$ film deposited on Si, after annealing for 20 minutes (sample S_1A_7).

Table 4 Surface roughness values (rms) of the investigated films

Sample	S_1	S_1A_2	S_1A_3	S_1A_4	S_1A_5	S_1A_6	S_1A_7	S_2A_6	S_3A_6
rms (nm)	1.34	3.6	5.4	15.48	18.7	33.75	9.17	41.6	54.29

The lower surface roughness of the films obtained under A_7 annealing condition is linked also with a dense structure, as observed by scanning electron microscopy (Fig. 8) in a cross-section for the S_1A_7 sample.

4. Conclusions

Tetragonal $Ba_6Mg_{0.67}Ta_{9.33}O_{30}$ thin films were obtained by magnetron sputtering method, using a single stoichiometric $Ba(Mg_{0.33}Ta_{0.67})O_3$ target, exhibiting a hexagonal crystallographic structure. The

measured bulk density of the $Ba(Mg_{0.33}Ta_{0.67})O_3$ target was ρ_r = 7.38 g/cm^3, with a total intergranular porosity of 3.1%.

The as deposited samples were amorphous, the films' crystallization taking place only at 900^{o}C annealing temperature, after several minutes.

The films' lattice parameters present larger values than those ascribed to the tetragonal BMT phase, indicating the inflation of the unit cell, due to the replacement of smaller Ba atoms with the larger Ta atoms. The best annealing condition were obtained for the samples introduced directly in the preheated oven. The ratios of different elements concentrations, as derived from XPS analyses, evidenced that the annealing process determines a Ba loss, inducing the tetragonal phase formation, as shown by XRD analysis.

The films morphology, as observed by AFM, presents a gradual increase of the surface roughness, as the duration of the annealing treatment is increased, due to film crystallization and growth of the grain dimensions. The higher deposition temperatures determined the increase of the surface roughness. The annealing treatments induced an increased roughness, the lower values being obtained for the films annealed with sudden temperature increase, which indicate this treatment to be more adequate for obtaining good quality films.

The deposited films present a compact, dense structure, specific for the magnetron sputtering deposition method. The presented results indicate that, in order to obtain stoichiometric and crystallized $Ba(Mg_{0.33}Ta_{0.67})O$ films, there is needed a second target, made by BaO, and an annealing treatment with a sudden temperature increase.

Acknowledgements

The work was supported by Romanian Ministry of Education and Research under the Project no. 71-040/2007.

References

[1] H. Matsumoto, H. Tamura, K. Wakino, Jpn. J. Appl. Phys. **30**(9B), 2347 (1991).
[2] S. B. Desu, H. M. O'Bryan, J. Am. Ceram. Soc. **68**(10), 546 (1985).
[3] Lai-Cheng Tien, Chen-Chia Chou, Dah-Shyang Tsai, Ceramics Int. **26,** 57 (2000).
[4] B. Vaidhanathan, D.K. Agrawal, T.R. Shrout, Y. Fang, Mater.Lett. **42** 207 (2000).
[5] S. Nomura, K. Kaneta, Japanese Journal of Applied Physics **33,** 507 (1984).
[6] T. Shimada, Journal of the European Ceramic Society **23,** 2647 (2003).
[7] Zhang Hui, Liu Zaiquan, Liu Hongfei, Fang Liang, Liu Hanxing, Journal of Wuhan University of Technology - Mater, **20**(3), 14 (2005)
[8] A. J. Moulson, J.M. Herbert, Electroceramics, Chapman and Hall, New York (1990).

[9] I-Nan Lin, Chen-Wei Liang, Ying-Hao Chu, Su-Jien Lin, J. Appl. Phys. **96**(10), 5701 (2004).
[10] Ji Zhou, Qing-Xin Su, K. M. Moulding, D. J. Barber, J. Mater. Res., **12**(3), 596 (1997).
[11] D. Ravichandran, R. Meyer Jr., R. Roy, R. Guo, A.S. Bhalla, L.E. Cross, Mat. Res.Bull. **31**(7), 817 (1996).
[12] B.W. Hakki, P.D. Coleman, IRE Transaction on Microwave Theory and Techniques, MTT **8,** 402 (1960).
[13] C. C. Negrila, C. Logofatu, R. V. Ghita, C. Cotarlan, F. Ungureanu, A.S.Manea, M.F.Lazarescu, J. Crystal Growth, **310,** 1576 (2008).
[14] C. C. Negrila ,C.Cotarlan, F.Ungureanu, C.Logofatu, R.V.Ghita, M.F.Lazarescu, J. Optoelectron. Adv. Mater. **10**(6) 1379 (2008).
[15] J. F. Moulder sa, Handbook of X-Ray Photoelectron Spectroscopy, Physical Electronics INC., 1992.
[16] C.D.Wagner, sa, Handbook of X-Ray Photoelectron Spectroscopy, Perkin-Elmer, 1979.
[17] B.V.Crist, Handbook of Monocromatic APS Spectra, XPS International, 1999.
[18] LASURFACE Database, www.lasurface.com/.
[19] NIST SRD20,Database Version 3.3.
[20] W.S. Choi, J.-H. Boo, J. Yi, B. Hong, Mat. Sci. Semicond. Proces., **5** 211 (2003) **.**
[21] Braic, M., Balaceanu, M., Vladescu, A., Kiss, A., Braic, V., Epurescu, G., Dinescu, G. Moldovan, A., Birjega, R., Dinescu, M., Appl. Surf. Sci. **253**(19), 8210 (2007).

*Corresponding author: mariana_braic@inoe.ro